

MAGNETISM OF ULTRAFINE PARTICLES

S. Gangopadhyay and G. C. Hadjipanayis

Department of Physics, University of Delaware, Newark, DE 19716

B. Dale and C.M. Sorensen

Department of Physics, Kansas State University, Manhattan, KS 66506

K. J. Klabunde

Department of Chemistry, Kansas State University, Manhattan, KS 66506

Introduction

The magnetic properties of ultrafine particles (UFP) are different from those in the bulk and they make them extremely important from the scientific and technological point of view. For example, ultrafine Fe particles are magnetically hard, with coercivity as high as 1.1kOe which is a few orders of magnitude higher than that of bulk Fe (1). UFPs can be prepared by various methods including chemical reduction (2), sputter deposition (3) and gas evaporation techniques (1,4,5). The magnetic properties of UFPs prepared by these techniques are very sensitive to the particle size. Therefore a good control of particle size is important for sample preparation. The particle size of evaporated particles depends on various factors such as: the pressure of the inert gas during evaporation, the atomic mass of inert gas, the evaporation temperature, the rate of evaporation and the substrate temperature.

In this paper we will report on the magnetic and structural properties of Fe, Co and Ni fine particles prepared by the gas evaporation technique. The effect of particle size and temperature on magnetization and coercivity has been studied. A correlation between microstructure and magnetic properties has been established in Fe particles using Mössbauer spectroscopy.

Experimental

In the evaporation-deposition technique, inert gas environment is required to form metal particles (in this study argon gas was used). Bulk metals of Fe, Co and Ni were evaporated from an alumina coated tungsten crucible in a glass bell-jar system. The system was first pumped down to $< 10^{-3}$ torr and then back filled with a continuous flow of argon. The range of gas pressure used for Fe and Co particles was 0.5-8.0 torr and for Ni particles 0.5-27 torr. The metal vapors suffer collisions with the argon molecules resulting in a decrease in their mean-free-path and form particles through the nucleation and growth process. These particles were collected on a water-cooled Cu substrate, whose typical distance from the boat was 2 cm. A carbon-coated Cu grid was used to collect samples for transmission electron microscopy. After evaporation the system was filled with an air-argon mixture for a few hours to passivate the surface of metal particles with their respective oxides.

The magnetic properties of the particles were measured with a SQUID magnetometer in the temperature range 10-300 K and in fields up to 55 kOe. X-ray diffractometry and transmission electron microscopy were used to determine the crystal structure and particle morphology.

Results and Discussion

1. Structural Properties

As mentioned in the earlier section, particle size and morphology play an important role in determining the magnetic properties of UFPs. The particle size was varied by varying the inert gas pressure. As the argon pressure increases the mean free path of the evaporated metal atoms decreases, giving them more time to form larger particles. This trend has been observed in all the three metal particles produced and is shown in Fig. (1) for Ni and Co particles. Particle sizes in the range 50-200 Å were obtained in the three systems studied. Each sample had a log-normal distribution in particle size. For Fe the standard deviation was in the range 1.1 - 1.3; for a 110 Å median diameter Ni particles, the standard deviation was 1.33. Particles obtained were nearly spherical for Fe and Co (Fig. (2)) but perfectly spherical in the case of Ni. The visually measured core size from bright field micrographs was in good agreement with that determined from the dark field micrographs.

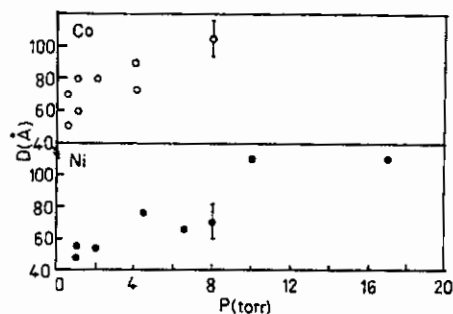


FIG. 1. Median diameter versus argon pressure in fine Ni and Co particles.

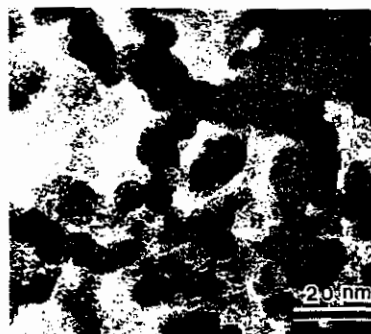


FIG. 2. Bright field micrograph of Fe particles with a median diameter 110 Å, showing the shell-type structure.

Selected area electron diffraction patterns and X-ray diffractometry showed the presence of α -Fe, γ -Fe₂O₃ and Fe₃O₄ in Fe particles; Ni and NiO in Ni particles; Co and CoO in Co samples. The diffraction lines were very sharp for bigger particles but broad in the smaller particles. The oxide lines were very broad and diffuse

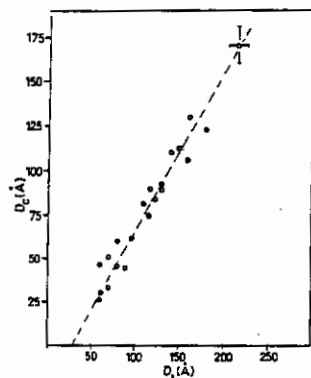


FIG. 3. Total median diameter versus core diameter for Fe. The slope of the straight line is 0.933 with a y-intercept of 26 Å.

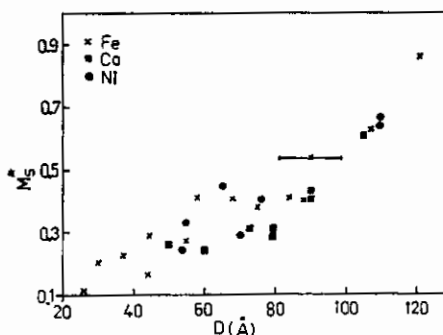


FIG. 4. $M_s^* = M_s(\text{sample at } T=10\text{K})/M_s(\text{bulk, at } T=0\text{ K})$ versus particle diameter.

indicating that the oxide calculate the core size of been established and is re increases linearly with a

2. Magnetic Properties

When the particles arerties significantly. For a surface coating two at Therefore the surface oxias the particle diameter i for Fe particles of diamete was 100 emu/g and 45 em attributed mainly to the

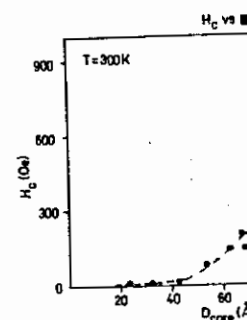


FIG. 5. Coercivity versus diameter D_{core} at $T = 300\text{ K}$.

The coercivity of fine p in coercivity with decreas diameter D_p , H_c is zero, demagnetize the sample.

indicating that the oxide coating is in the form of very small crystallites. A detailed study has been made to calculate the core size of Fe particles. An empirical relation between the core diameter and outer diameter has been established and is reported elsewhere (4). It is observed that as the outer diameter increases the core also increases linearly with a negative intercept as shown in Fig. (3).

2. Magnetic Properties

When the particles are smaller the surface effects are more dominant and these affect their magnetic properties significantly. For a particle of 25 Å diameter more than 50% of the atoms lie on the surface (assuming a surface coating two atomic layers thick); whereas for a particle of 150 Å diameter, this fraction is only 8%. Therefore the surface oxidation effects are much more pronounced in the smaller particles. Fig. (4) shows that as the particle diameter increases the normalized magnetization ratio also increases reaching a maximum of 0.9 for Fe particles of diameter 130 Å. The maximum magnetization (at $H = 55$ kOe) achieved for Co and Ni particles was 100 emu/g and 45 emu/g, respectively. The reduction of magnetization in the smaller particles has been attributed mainly to the surface oxidation effects.

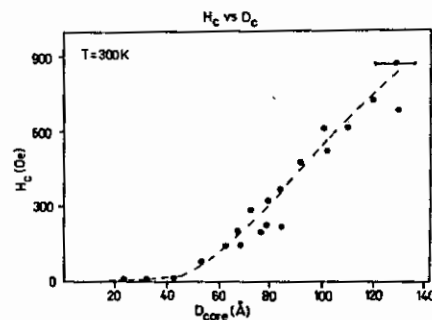


FIG. 5. Coercivity versus particle diameter at $T = 300$ K.

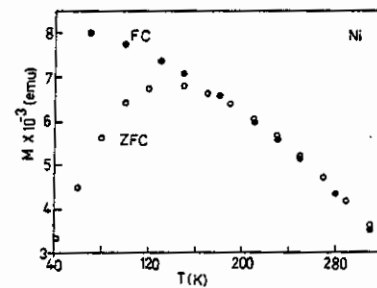


FIG. 6. Thermomagnetic data for Ni particle with diameter 55 Å.

TABLE 1

	Median Particle Diameter D (Å)	T_B (K)
Fe:	90	310
	65	170
	60	150
Ni:	110	>300
	76	200
	55	150

The coercivity of fine particles has a strong dependence on the particle size as is shown in Fig. 5. The decrease in coercivity with decreasing particle size in the single domain region is due to thermal effects. Below a critical diameter D_p , H_c is zero, because the thermal effects are strong enough to overcome the anisotropy energy and demagnetize the sample. Such particles are referred to as superparamagnetic. But at 10 K where the thermal

ant role in determining the gas pressure. As the argon ng them more time to form ed and is shown in Fig. (1) hree systems studied. Each n was in the range 1.1 - 1.3; icles obtained were nearly lly measured core size from rk field micrographs.



of Fe particles with a the shell-type structure.

presence of α -Fe, γ -Fe₂O₃. The diffraction lines were very broad and diffuse



$M/M_s(\text{bulk, at } T=0 \text{ K})$

energy is negligible, the coercivity was found to increase with the particle diameter decreased. This might be due to the larger surface anisotropy effects in smaller particles. The temperature at which superparamagnetic behavior is observed is known as the blocking temperature (T_B). The superparamagnetic transition is also seen in the field cooled thermomagnetic data which exhibited a peak near T_B (Fig. (6)). The relation between blocking temperature and particle diameter is shown in Table 1. Both Fe and Ni particles with a size below 70 Å show superparamagnetic effects. No superparamagnetism was observed in Co in particles with a diameter below 70 Å.

The temperature dependence of coercivity is shown in Fig. 7. In the smaller particles, the decrease in coercivity with temperature is very drastic as compared to that of bigger particles (Fig. 7). This temperature dependence can be explained by considering the Mössbauer spectra of an Fe sample ($D = 130$ Å) in the temperature range 4.2–300 K, shown in Fig. (8). Above 85 K the hyperfine magnetic splitting due to α -Fe is superimposed on a broad peak due to the superparamagnetic Fe-oxide coating. The presence of a broad peak instead of a quadrupole splitting for the superparamagnetic oxide coating has been attributed to the interaction between the magnetic core and the surface oxide shell (5-7). At low temperatures both the particle core and coating are magnetically hard. But as the temperature is increased above 85 K, the magnetic moment of the oxide fluctuates randomly. This causes the Fe core to become magnetically softer in the smaller particles because most of the Fe atoms are very close to the surface. For example Fe particles with diameter 60 Å showed a negligible coercivity at 150 K which increased to 3400 Oe at 10 K. In larger particles the volume fraction of oxide is much smaller and does not affect the behavior of the Fe core significantly. The Fe particles with median diameter of 130 Å showed an H_c of 507 Oe at 300 K which increased to 1613 Oe at cryogenic temperatures.

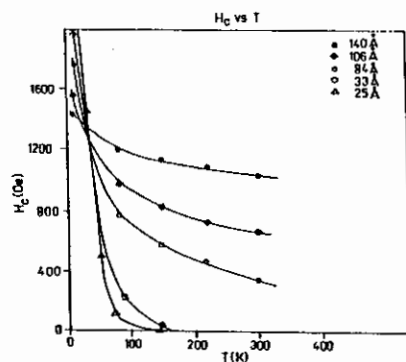


FIG. 7. Coercivity versus temperature for different size particles.

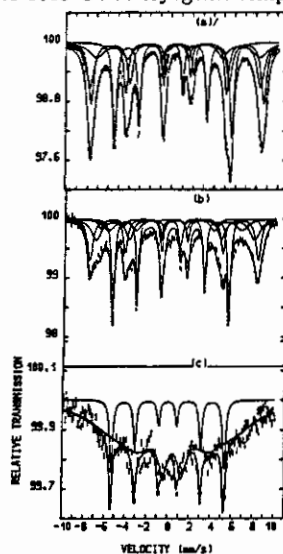


FIG. 8. Mössbauer spectra of Fe at (a) $T = 4.2$ K, (b) $T = 85$ K, (c) $T = 300$ K.

The large value of coercivity obtained in fine particles is not well understood yet. The largest H_c obtained for Fe, Co and Ni at room temperature were 1050, 1200 and 100 Oe, respectively. It was found that the value of effective anisotropy K for Fe particles was an order of magnitude higher than that of bulk Fe. Since these particles have negligible shape anisotropy, the main contribution to anisotropy energy could be from: (1) magnetocrystalline anisotropy, (2) surface anisotropy and (3) metal-oxide interface coupling. We are presently trying to modify the surface of these particles by coating them with materials other than oxides, to investigate further the effect of surface on their magnetic hysteresis behavior.

Ultrafine particles

The magnetic properties of ultrafine particles of Fe, Co, Ni were 1050, 1200 and 100 Oe, respectively. The magnetic and Mössbauer spectra of these particles are shown in Fig. 7. The value of coercivity is very low.

This work has been supported by the National Science Foundation at Demokritos.

1. A. Tasaki, M. Takasaka, and T. Kikuchi.
2. L. Yiping, G. C. Han, and J. H. W. Lam.
3. G. Xiao, C. L. Chien, and J. H. W. Lam.
4. S. Gangopadhyay, C. L. Chien, and J. H. W. Lam.
5. V. Papaefthymiou, J. Klabunde, and C. M. Sotomayor.
6. I. Tamura and M. H. Sato.
7. K. Haneda and A. Tasaki.

Conclusion

Ultrafine particles of Fe, Co and Ni were successfully made with a particle size in the range of 50-200Å. The magnetic properties were found to depend strongly on particle size with the smaller particles of Fe and Ni showing superparamagnetism at low temperatures. The highest coercivities obtained at room temperature for Fe, Co, Ni were 1050, 1200 and 100 Oe, respectively. A correlation of transmission electron microscopy data with the magnetic and Mössbauer measurements indicated a shell-type structure in these particles with a metal core surrounded by an oxide coating. Further surface studies are needed in order to understand and explain the high value of coercivity.

Acknowledgements

This work has been supported by NSF-CHE-8706954. We would like to thank Dr. Kostikas and Dr. Papaefthymiou at Demokritos, Athens, Greece for their help in the Mössbauer studies.

References

1. A. Tasaki, M. Takao and H. Tokunaga, J. J. Appl. Phys. **13**, 271 (1974).
2. L. Yiping, G. C. Hadjipanayis, C. M. Sorensen and K. L. Klabunde, J. Mag. Magn. Mat. **79**, 321 (1989).
3. G. Xiao, C. L. Chien, J. Appl. Phys. **51**, 1280 (1987).
4. S. Gangopadhyay, G. C. Hadjipanayis (submitted to Phys. Rev. B).
5. V. Papaefthymiou, A. Kostikas, A. Simopoulos, D. Niarchos, S. Gangopadhyay, G. C. Hadjipanayis, K. J. Klabunde and C. M. Sorensen, J. Appl. Phys. **67**(a), 4487 (1990).
6. I. Tamura and M. Hayashi, Surf. Sci. **146**, 501 (1984).
7. K. Haneda and A. H. Morrish, Nature **282**, 186 (1979).